IJAREEIE

e-ISSN: 2278-8875
p-ISSN: 2320-3765

International Journal of Advanced Research in Electrical, Electronics and Instrumentation Engineering

Volume 13, Issue 12, December 2024

INTERNATIONAL STANDARD SERIAL NUMBER INDIA

Impact Factor: 8.514

International Journal of Advanced Research in Electrical, Electronics and Instrumentation Engineering (IJAREEIE)

| e-ISSN: 2278 – 8875, p-ISSN: 2320 – 3765| www.ijareeie.com | Impact Factor: 8.514 | A Monthly Peer Reviewed & Refereed Journal |

|| Volume 13, Issue 12, December 2024 ||

| DOI:10.15662/IJAREEIE.2024.1312010 |

Design of Improved Voltage Gain by Hybrid Non-Isolated Bidirectional Dc-Dc Converter

R. Aravind Kumaran, V. Geetha

PG Student (PED), Dept. of EEE, Government College of Engineering, Salem, Tamil Nadu, India

Professor and Head, Dept. of EEE, Government College of Engineering, Salem, Tamil Nadu, India

ABSTRACT: An overview of the Hybrid Non-Isolated Bidirectional DC-DC Converter, which is especially designed for EV charging and discharging from the DC grid, is presented in this design to analyse and identify the existing converter topology's issues. In order to charge EVs and feed energy back into the grid, it creates a bi-directional architecture that permits energy to flow both ways. In order to increase the voltage gain, the updated circuit uses buck boost converters, four switches with body diodes, passive components like two inductors, and a capacitor. For energy storage, high voltage conversion ratio, and EV charging applications, this design is an excellent choice. To validate the converter's performance, extensive simulations are carried out using MATLAB/SIMULINK with suitable parameters. The simulation results demonstrate the converter's ability and high performance for the charging of EV batteries.

KEYWORDS: Bidirectional, Hybrid, Voltage Gain

I. INTRODUCTION

Green Energy Sources (GES) are becoming more popular as a way to lower carbon emissions and footprints. GES's input power fluctuation, however, essentially does not compete with users' power consumption. As a result, this raises issues with stability and dependability in the electrical grid network. Solar and wind-powered autonomous generation systems are widely utilized to power a variety of appliances, buildings, and systems as well as to provide heating, lighting, and other functions in practically every industry. Super-capacitors, accumulators (batteries), or various energy buffers are used by nearly all of these systems to provide steady functioning under all circumstances and demands.

Governments and the commercial sector are being pushed to reduce their dependency on fossil fuels and make investments in the electric vehicle (EV) industry by the escalating environmental pollution and the exacerbated issue of global warming. One of the system's components is the bidirectional DC–DC converter, which connects RES-based power generation to storage systems (in charge mode) and transfers storage power to the DC/AC inverter or DC load (in discharge mode). To control power processing during the switch from storage systems to load and overload, a bidirectional DC–DC converter is also necessary. Depending on the mode of operation, the bidirectional DC–DC converter can be utilized in systems that need current to flow in both directions. These converters are widely employed for a variety of environmentally friendly green energy applications and are essential components of energy backup systems.

These converters achieve better performance characteristics by combining the benefits of several topologies, including buck, boost, and buck-boost. Hybrid converters can provide greater efficiency, lower component stress, and wider voltage gain ranges by utilizing the advantages of each design. A greater range of voltage ratios can be achieved by hybrid topologies, which makes them appropriate for a number of applications. Hybrid converters can attain great efficiency, particularly at high power levels, by minimizing conduction losses and improving switching patterns. Non-isolated topologies can be more affordable and smaller due to the removal of the isolation transformer, which makes them appealing for applications where cost is a concern. The lifespan of the converter can be increased and component failure risk reduced by distributing voltage and current stressors among several components. Multi-level, switched-capacitor,

| e-ISSN: 2278 – 8875, p-ISSN: 2320 – 3765| www.ijareeie.com | Impact Factor: 8.514 | A Monthly Peer Reviewed & Refereed Journal |

|| Volume 13, Issue 12, December 2024 ||

| DOI:10.15662/IJAREEIE.2024.1312010 |

CUK/CUK, SEPIC/ZETA, buck-boost, coupled-inductor, three-level, and traditional buck/boost are variants of non-isolated types. More switches and capacitors are needed in multi-level and switched-capacitor kinds if a high voltage gain is needed. These kinds of control circuits are also complex.

II. PROPOSED SYSTEM

HYBRID DC-DC CONVERTER:

A promising method for successfully overcoming the obstacles is the use of hybrid DC–DC converters. Multiple converter topologies or approaches are combined in hybrid DC–DC converters to accomplish particular performance goals. These hybrid solutions maximize efficiency, voltage regulation, power density, and other required attributes by combining the benefits of various converter types.

Table 1. Hybrid DC-DC Converters and Topologies

HYBRID DC-DC CONVERTER	TOPOLOGIES COMBINED
Buck-Boost Converter	Buck, Boost
SEPIC-Cuk Converter	SEPIC, Cuk
Flyback-Forward Converter	Flyback, forward
Full-Bridge LLC Converter	Full-Bridge, LLC
Hybrid Multilevel Converter	Various multilevel topologies
Flyback-Cuk Converter	Flyback, CuK
Flyback-SEPIC Converter	Flyback, SEPIC

BIDIRECTIONAL DC-DC CONVERTER:

A bidirectional converter is a power electronic device that can facilitate the flow of electrical power in both directions. Unlike traditional unidirectional converters, which only allow power to flow in one direction, bidirectional converters offer flexibility and efficiency in various applications. By strategically controlling the switching patterns of the power electronic devices, the converter can either step up or step down the voltage, or even reverse the direction of power flow. Bidirectional converters enable the charging of the vehicle's battery from the grid and also allow the vehicle to feed power back to the grid (vehicle-to-grid, or V2G). They enable the charging and discharging of batteries, optimizing energy storage and utilization.

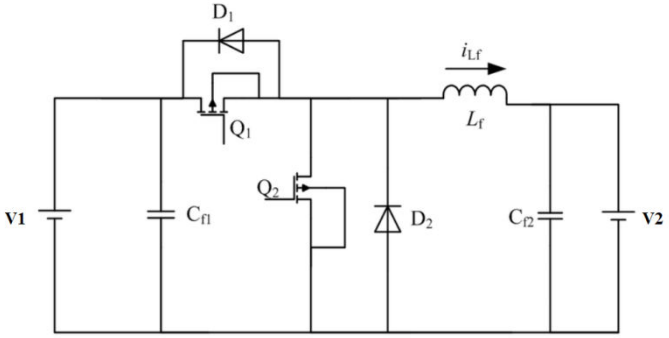

Figure 1. Basic Circuit of Bidirectional DC-DC Converter

Bidirectional DC–DC converters are available in two configurations: isolated topology and non-isolated topology. Magnetic isolation separates the power transfer between the input and output in an isolated topology. Non-isolated topology, on the other hand, does not involve isolation. The non-isolated conventional bidirectional DC–DC converter's primary and simplest topology is the buck–boost bidirectional converter. When charging the storage systems, the converter runs in buck mode. When discharging electricity to meet the DC/DC voltage needs, it functions in boost mode.

| e-ISSN: 2278 – 8875, p-ISSN: 2320 – 3765| www.ijareeie.com | Impact Factor: 8.514 | A Monthly Peer Reviewed & Refereed Journal |

|| Volume 13, Issue 12, December 2024 ||

| DOI:10.15662/IJAREEIE.2024.1312010 |

III. CIRCUIT DIAGRAM AND OPERATION

Figure 2 displays the converter's anticipated topology. It has two inductors, a capacitor, and four power switches with body diodes. In these works, two inductors with different values are implemented, resulting in differing currents when compared to the inductor value in the converter. During step-up operation, the two boost converters created by this topology's two inductors increase their voltage gain. The current in one of the switches is simultaneously the high sum of the two inductor currents during step-down operation. The relevant switch's switching losses are significantly decreased by employing synchronous rectification, which raises efficiency.

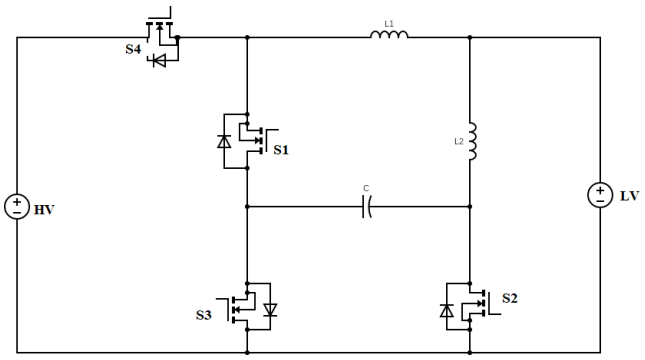

Figure 2. Circuit Diagram of Proposed System

The steady-state analysis for the boost and buck modes of operation have been conducted under the following presumptions. The equivalent series resistance of the inductors and capacitor is disregarded for the ON-state resistance RDS (ON) of the power switches, and the voltage across the capacitor is taken to be constant. The switches S_3 and S_4 are controlled simultaneously using the pulse width modulation (PWM) technique. The S_1 and S_2 switches function as synchronous rectifiers.

MODES OF OPERATION:

There are two modes of operation in this proposed system. They are

1. Step – Down Operation
2. Step – Up Operation

STEP – DOWN OPERATION:

Figure 3 shows the circuit of the proposed topology in step-down operation; S1 and S2 serve as synchronous rectifiers and S3 and S4 as control switches. Depending on when the associated switches are triggered, it can operate in two different states.

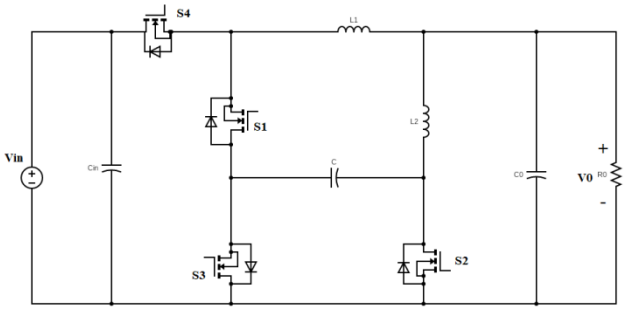

Figure 3. Step-Down Operation

STATUS – I ($t_0 \leq t \leq t_1$)

During this time span, the switches S_3 and S_4 are turned ON, while the switches S_1 and S_2 turned OFF at the same time by means of applying the gate pulses to the appropriate switches. The energy from the high-voltage end, which is the input voltage V_{in}, is transferred on the way to the inductor L_1.The capacitor C is discharged through inductor L_2 and capacitor C_0.

| e-ISSN: 2278 – 8875, p-ISSN: 2320 – 3765| www.ijareeie.com | Impact Factor: 8.514 | A Monthly Peer Reviewed & Refereed Journal |

|| Volume 13, Issue 12, December 2024 ||

| DOI:10.15662/IJAREEIE.2024.1312010 |

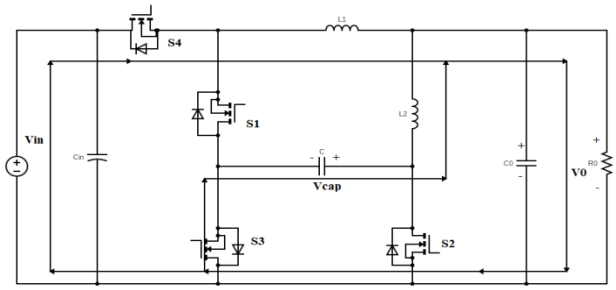

Figure 4. Status – I

Thus the inductor voltages in L_1 and L_2 are attained as

$$\boldsymbol{V_{L1} = V_{in} - V_0} \quad (1)$$
$$\boldsymbol{V_{L2} = V_{Cap} - V_0} \quad (2)$$

STATUS II ($t_1 \leq t \leq t_2$)

During this time span, the switches S1 and S2 are turned ON, while switches S3 and S4 are turned OFF, by means of applying the gate pulses to the appropriate switches. The inductor L_1 is demagnetized to capacitors C and C_0. The inductor energy stored in L_2 is released to capacitor C_0, which provides energy to the load. Therefore, the inductor voltages can be expressed as

$$\boldsymbol{V_{L1} = -V_0 - V_{Cap}} \quad (3)$$
$$\boldsymbol{V_{L2} = -V_0} \quad (4)$$

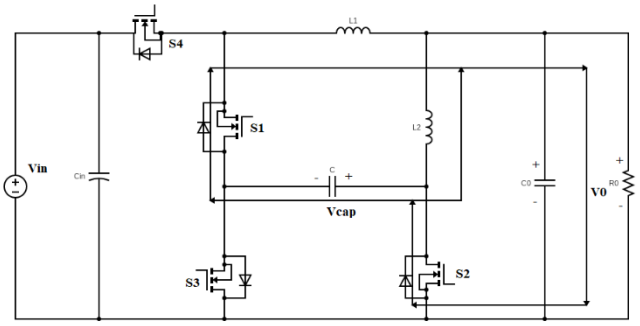

Figure 5. Status - II

Applying the technique of voltage-second (V-S) balance on the inductors L_1 and L_2, we obtain,

$$\langle \boldsymbol{V_{L1}} \rangle = \int_0^{DT_s} (\boldsymbol{V_{in} - V_0})\boldsymbol{dt} + \int_{DT_S}^{T_s} (\boldsymbol{-V_0 - V_{Cap}})\boldsymbol{dt} = \boldsymbol{0} \quad (5)$$
$$\langle \boldsymbol{V_{L2}} \rangle = \int_0^{DT_s} (\boldsymbol{V_{Cap} - V_0})\boldsymbol{dt} + \int_{DT_S}^{T_s} (\boldsymbol{-V_0})\boldsymbol{dt} = \boldsymbol{0} \quad (6)$$

Hence, the voltage gain of step-down under continuous conduction mode specified by

$$\boldsymbol{G_{CCM(step-down)} = \frac{V_0}{V_{in}} = D^2} \quad (7)$$

If the inductors are operated under boundary condition mode (BCM), then the capacitors Cap and C_0 currents are expressed as

$$i_{Cap} = \{-I_{L2} \quad 0 \leq t \leq DT_S$$
$$\boldsymbol{i_{Cap} = \{I_{L1} \quad DT_S \leq tT_s} \quad (8)$$

| e-ISSN: 2278 – 8875, p-ISSN: 2320 – 3765| www.ijareeie.com | Impact Factor: 8.514 | A Monthly Peer Reviewed & Refereed Journal |

|| Volume 13, Issue 12, December 2024 ||

| DOI:10.15662/IJAREEIE.2024.1312010 |

The current of the capacitor C_0 is $I_{L1} + I_{L2} - I_0$. Applying the technique of A-S (ampere-second) balance on the capacitors, Cap and C_0,

$$\langle i_{Cap} \rangle = 0 = \frac{-DT_S I_{L2} + (1-D)T_S I_{L1}}{T_S} \Longrightarrow I_{L1} = \frac{D}{(1-D)} I_{L2} \quad (9)$$

$$\langle i_{Cap} \rangle = 0 \Longrightarrow I_{L1} + I_{L2} - I_0 \quad (10)$$

Therefore, the average currents of the inductors are

$$I_{L1} = DI_0 \quad (11)$$

$$I_{L2} = (1-D)I_0 \quad (12)$$

Current ripples of the inductors L_1 and L_2 can be attained as from the integral form of the current expressions of the inductors L_1 as well as L_2.

$$i_{L1}(DT_S) = i_{L1}(0) + \frac{1}{L_1}\int_0^{DT_S} V_{L1}(t)dt \Longrightarrow \Delta i_{L1} = \frac{D(V_{in}-V_0)}{L_1 f_{SW}} \quad (13)$$

$$i_{L2}(DT_S) = i_{L2}(0) + \frac{1}{L_2}\int_0^{DT_S} V_{L2}(t)dt \Longrightarrow \Delta i_{L2} = \frac{D(V_{Cap}-V_0)}{L_2 f_{SW}} \quad (14)$$

Express the inductor values as

$$I_{L1} \geq \frac{1}{2}\Delta i_{L1}$$

$$I_{L2} \geq \frac{1}{2}\Delta i_{L2}$$

Determine the value of L_1,

$$DI_0 \geq \frac{D(V_{in} - V_0)}{2L_1 f_{SW}}$$

Where,

$$I_0 = \frac{V_0}{R_0}; \frac{V_{Cap}}{V_{in}} = \frac{V_0}{V_{Cap}} = D$$

The expression becomes

$$D\frac{V_0}{R_0} = \frac{D(V_{in} - V_0)}{2L_1 f_{SW}}$$

Similarly, for the inductor value L_2,

$$(1-D)I_0 \geq \frac{D(V_{Cap} - V_0)}{2L_2 f_{SW}}$$

$$\frac{(1-D)V_0}{R_0} \geq \frac{D(V_{Cap} - V_0)}{2L_2 f_{SW}}$$

After simplification of the above Equations, the least possible values of inductors can be expressed as

$$L_1 \geq \frac{(1-D^2)R_0}{2D^2 f_{SW}} \quad (15)$$

$$L_2 \geq \frac{R_0}{2f_{SW}} \quad (16)$$

STEP – UP OPERATION:

The circuit of proposed topology in step-up operation is illustrated in Figure 6; Here, S1 and S2 act as control switches and S3 and S4 are synchronous rectifiers. It operates under two statuses based on the triggering of the corresponding switches.

| e-ISSN: 2278 – 8875, p-ISSN: 2320 – 3765| www.ijareeie.com | Impact Factor: 8.514 | A Monthly Peer Reviewed & Refereed Journal |

|| Volume 13, Issue 12, December 2024 ||

| DOI:10.15662/IJAREEIE.2024.1312010 |

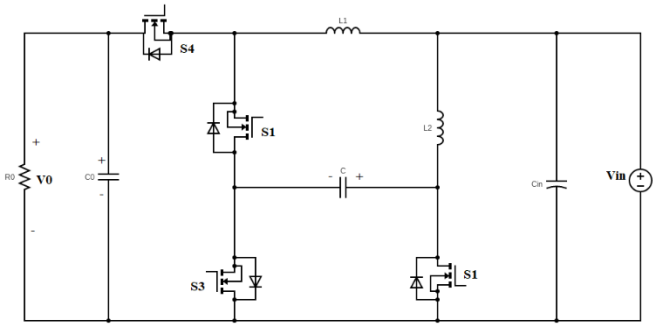

Figure 6. Step – Up Operation

STATUS – I ($t_0 \leq t \leq t_1$)

During this time span, the switches S_1 and S_2 are turned ON, while the switches S_3 and S_4 turned OFF at the same time by means of applying the gate pulses to the appropriate switches. The energy from the low-voltage end, which is the input voltage V_{in}, is transferred on the way to the inductor L_2. Inductor L_1 is magnetized by the input DC source V_{in} and the energy stored in capacitor C.

Hence the voltages across the inductors L_1 and L_2 are expressed as

$$V_{L1} = V_{in} + V_{Cap} \quad (17)$$

$$V_{L2} = V_{in} \quad (18)$$

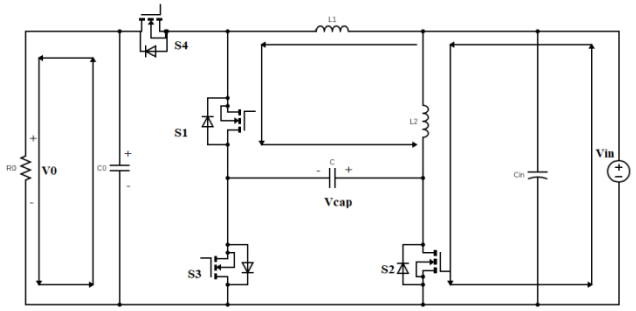

Figure 7. Status – I

STATUS II ($t_1 \leq t \leq t_2$)

During this time span, the switches S_1 and S_2 are turned OFF, while switches S_3 and S_4 turned ON at the same time by means of applying the gate pulses to the appropriate switches. The capacitor C is charged by the input supply, V_{in}, and the energy stored in inductor L_2. Capacitor C_0 is also charged by the input supply, V_{in}, and the energy stored in inductor L_1.

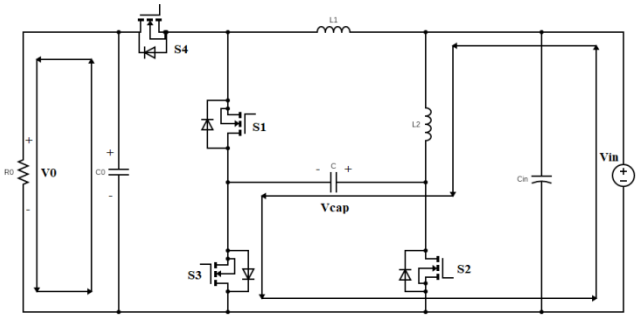

Figure 8. Status II

| e-ISSN: 2278 – 8875, p-ISSN: 2320 – 3765| www.ijareeie.com | Impact Factor: 8.514 | A Monthly Peer Reviewed & Refereed Journal |

|| Volume 13, Issue 12, December 2024 ||

| DOI:10.15662/IJAREEIE.2024.1312010 |

The inductor voltages across L1 and L2 are expressed as

$$\boldsymbol{V_{L1} = V_{in} - V_0} \quad (19)$$

$$\boldsymbol{V_{L2} = V_{in} - V_{Cap}} \quad (20)$$

According to the voltage-second (V-S) balance technique applied to the inductors, its further generalization produces the Equation for step-up gain in continuous conduction mode (CCM) as exemplified by the following expressions:

$$\boldsymbol{\int_0^{DT_S}(V_{in} + V_{Cap})dt + \int_{DT_s}^{T_S}(V_{in} - V_0)dt = 0} \quad (21)$$

$$\boldsymbol{\int_0^{DT_S} V_{in}dt + \int_{DT_S}^{T_S}(V_{in} - V_{Cap})dt = 0} \quad (22)$$

$$\boldsymbol{G_{CCM(step-up)} = \frac{V_0}{V_{in}} = \frac{1}{(1-D)^2}} \quad (23)$$

The C and C_0 capacitor currents are expressed as

$$i_{Cap} = \{-I_{L1} \quad 0 \le t \le DT_S$$

$$i_{Cap} = \{I_{L2} \quad DT_S \le t \le T_S \quad (24)$$

$$i_{C_0} = \{-I_0 \quad 0 \le t \le DT_S$$

$$i_{C_0} = \{I_{L1} - I_0 \quad DT_S \le t \le T_S \quad (25)$$

By using the ampere-second balance principle on C and C_0,

$$\langle i_{Cap} \rangle = 0 = \frac{-DT_S I_{L1} + (1-D)T_S I_{L2}}{T_S} \Longrightarrow I_{L2} = \frac{D}{(1-D)} I_{L1} \quad (26)$$

$$\boldsymbol{\langle i_{C_0} \rangle = 0 = I_{L1} = \frac{1}{(1-D)} I_0} \quad (27)$$

$$\boldsymbol{I_{L2} = \frac{D}{(1-D)^2} I_0} \quad (28)$$

The expression for the inductor current ripples in L_1 and L_2 are written as

$$\boldsymbol{i_{L1}(DT_S) = i_{L1}(0) + \frac{1}{L_1}\int_0^{DT_S} V_{L1}(t)dt \Longrightarrow \Delta i_{L1} = \frac{D(V_{in}+V_{Cap})}{L_1 f_{SW}}} \quad (29)$$

$$\boldsymbol{i_{L2}(DT_S) = i_{L2}(0) + \frac{1}{L_2}\int_0^{DT_S} V_{L2}(t)dt \Longrightarrow \Delta i_{L2} = \frac{DV_{in}}{L_2 f_{SW}}} \quad (30)$$

The converter operates under CCM, when the average value of an inductor is more than half of its current ripples. The inductor values based on its ripples are expressed as

$$\boldsymbol{I_{L1} \ge \frac{1}{2}\Delta i_{L1}}$$

$$\boldsymbol{I_{L2} \ge \frac{1}{2}\Delta i_{L2}}$$

For determining the value of L_1,

$$\frac{I_0}{1-D} \ge \frac{D(V_{in} + V_{Cap})}{2L_1 f_{SW}}$$

where

$$I_0 = \frac{V_0}{R_0}; \frac{V_{Cap}}{V_{in}} = \frac{V_0}{V_{Cap}} = \frac{1}{1-D}$$

The expression becomes

$$\frac{V_0}{R_0(1-D)} = \frac{D(2-D)V_{Cap}}{2L_1 f_{SW}}$$

Similarly, for the inductor value L_2,

| e-ISSN: 2278 – 8875, p-ISSN: 2320 – 3765| www.ijareeie.com | Impact Factor: 8.514 | A Monthly Peer Reviewed & Refereed Journal |

|| Volume 13, Issue 12, December 2024 ||

| DOI:10.15662/IJAREEIE.2024.1312010 |

$$\frac{DI_0}{(1-D)^2} \geq \frac{DV_{in}}{2L_2 f_{SW}}$$

$$\frac{V_0}{R_0(1-D)^2} \geq \frac{V_{in}}{2L_2 f_{SW}}$$

After simplification of the above expressions, the least possible values of inductors can be found as

$$\boldsymbol{L_1 \geq \frac{D(2-D)(1-D)^2 R_0}{2f_{SW}}} \quad (31)$$

$$L_2 \geq \frac{(1-D)^4 R_0}{2f_{SW}} \quad (32)$$

If the values of the inductors are less than the above expression, then the converter will face the boundary condition or even the discontinuous conduction mode.

V. SIMULATION AND RESULTS

The simulation circuit of the proposed system is shown in figure 9. The simulation is done in MATLAB 2023A version with ode45 solver. The Discrete powergui with a value of 1 μs is used to run the simulation and visualize the results. The proposed converter is provided in open loop control for getting better performance.

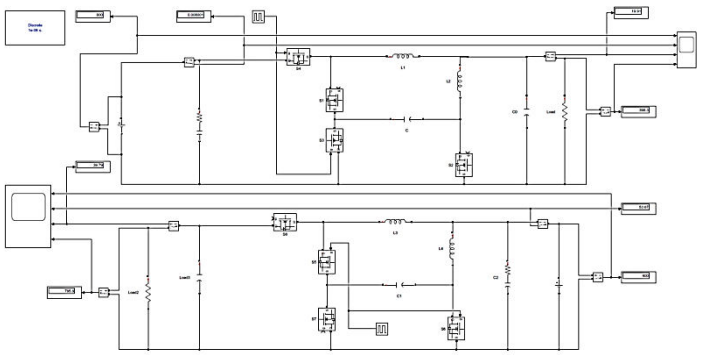

Figure 9. Simulation Circuit

In this circuit, there are two separate circuits are shown. It shows the bidirectional working of the converter. In the circuit, the above one shows the step-down operation of the power converter and the below one shows the step-up operation of the power converter.

POWER FLOW IN STEP-DOWN OPERATION:

In the figure 10 shows the simulation circuit of the step-down operation of the bidirectional converter of the proposed system. In this circuit it shows the power flow from high voltage side (Eg. DC Grid) to the low voltage side.

This circuit is made for the charging purpose of the battery in the electric vehicle.

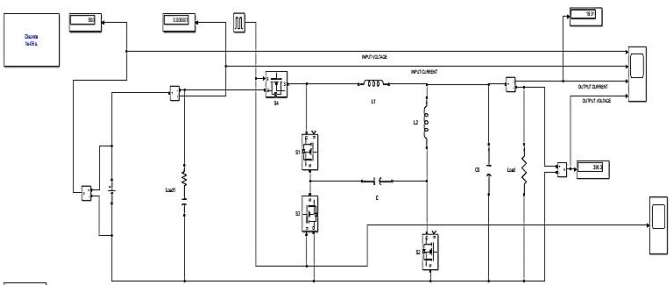

Figure 10. Step-Down Operation

| e-ISSN: 2278 – 8875, p-ISSN: 2320 – 3765| www.ijareeie.com | Impact Factor: 8.514 | A Monthly Peer Reviewed & Refereed Journal |

|| Volume 13, Issue 12, December 2024 ||

| DOI:10.15662/IJAREEIE.2024.1312010 |

SWITCHING PULSE & OUTPUT WAVEFORM:

Switching pulse for the step-down operation is shown the figure 11. It shows the pulse for the switch S3 and S4 of the converter. This is for the switch turn ON and OFF time of the converter.

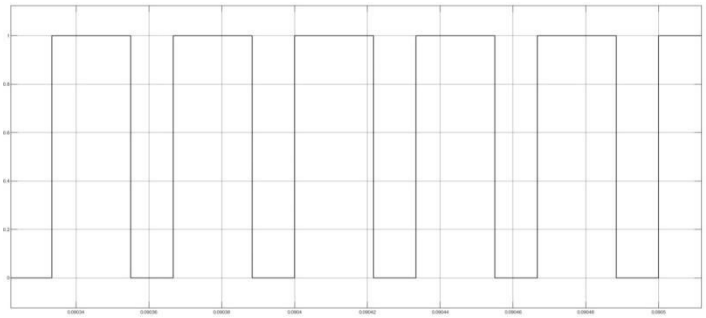

Figure 11. Switching pulse of Step-down Operation

From the simulation of the step-down operation, the results are displayed in the figure 12. It shows the waveforms of input voltage V_{in}, input current I_{in}, output voltage V_0 and output current I_0.

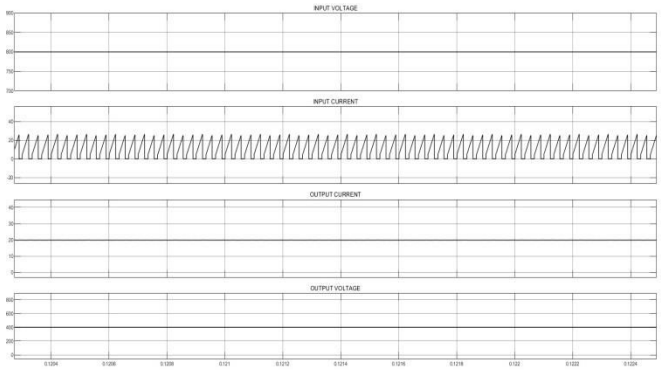

Figure 12. Input and Output Waveforms of Step-down Operation

POWER FLOW IN STEP-UP OPERATION:

In the figure 13 shows the simulation circuit of the step-down operation of the bidirectional converter of the proposed system. In this circuit it shows the power flow from low voltage side (Eg. EV Battery) to the high voltage side. This circuit is made for the discharging purpose of the battery in the electric vehicle.

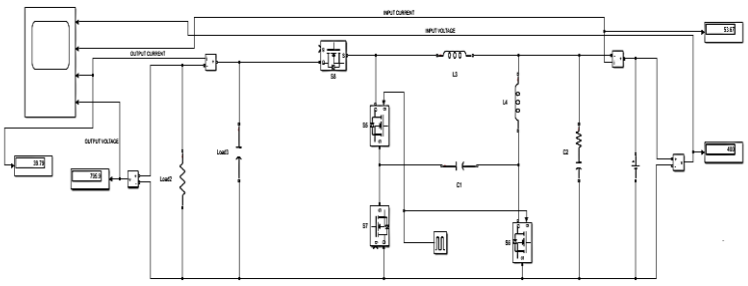

Figure 13. Step-Up Operation

| e-ISSN: 2278 – 8875, p-ISSN: 2320 – 3765| www.ijareeie.com | Impact Factor: 8.514 | A Monthly Peer Reviewed & Refereed Journal |

|| Volume 13, Issue 12, December 2024 ||

| DOI:10.15662/IJAREEIE.2024.1312010 |

SWITCHING PULSE & OUTPUT WAVEFORM:

Switching pulse for the step-up operation is shown the figure 6.6. It shows the pulse for the switch S1 and S2 of the converter. This is for the switch turn ON and OFF time of the converter.

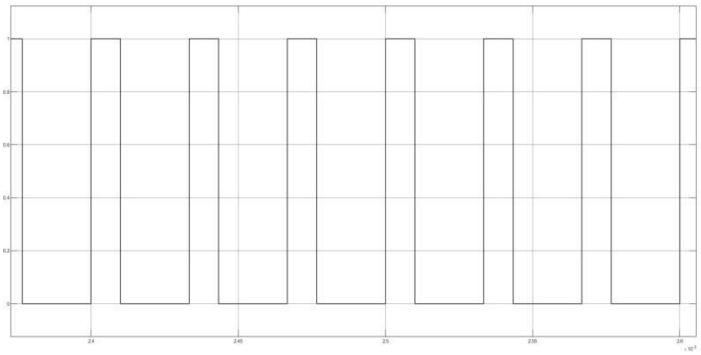

Figure 14. Switching Pulse of Step-Up Operation

From the simulation of the step-up operation, the results are displayed in the figure 6.7. It shows the waveforms of input voltage V_{in}, input current I_{in}, output voltage V_0 and output current I_0.

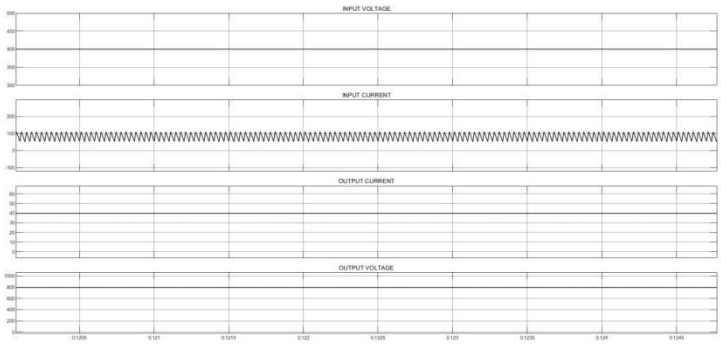

Figure 15. Input and Output Waveforms of Step-up Operation

SIMULATION PARAMETERS:

TABLE 2. Simulation Parameter for Step-Down & Step-Up Operation

PARAMETERS	SPECIFICATIONS	
	STEP-DOWN	STEP-UP
INPUT VOLTAGE	800	400
OUTPUT VOLTAGE	400	800
OUTPUT CURRENT	20	40
DUTY CYCLE	65%	30%
INDUCTOR L_1	400 μH	400 μH
INDUCTOR L_2	104 μH	104 μH
OUTPUT CAPACITOR	420 μF	420 μF

VI. CONCLUSION

This project successfully demonstrates the design of hybrid non-isolated bidirectional DC-DC converter. The suggested system incorporates modern power conversion methods to guarantee effective and bidirectional power flow,

| e-ISSN: 2278 – 8875, p-ISSN: 2320 – 3765| www.ijareeie.com | Impact Factor: 8.514 | A Monthly Peer Reviewed & Refereed Journal |

|| Volume 13, Issue 12, December 2024 ||

| DOI:10.15662/IJAREEIE.2024.1312010 |

which is necessary for high voltage gain, bidirectional battery charging, and contemporary EV systems. When compared to traditional converters, the suggested architecture yields a large voltage gain during both step-up and step-down operations. The input current splits between the two inductors during step-up operation, increasing the voltage gain. The efficiency is increased because the total of the two inductor currents produces a high output current as a result of the switches' synchronous rectification during step-down operation. As a result, battery charging applications with a lower output voltage and a higher current are best suited for the suggested design. Future research can concentrate on hardware implementation for experimental validation in order to evaluate operational difficulties and practical performance. Furthermore, incorporating cutting-edge control techniques like AI-based adaptive or predictive control may improve the system's dynamic reaction, stability, and efficiency even more. In addition to addressing greater voltage levels and lowering switching losses, investigating multilayer converter topologies may make them appropriate for a wider variety of EV applications. Battery life can be increased and state-of-charge management optimized with additional integration with Battery Management Systems (BMS). The sustainability of EV systems may also be improved by modifying the design to be compatible with renewable energy sources like solar and wind power. Finally, this study is expanding this technology for different EV configurations, such as heavy-vehicles, cars and two-wheelers, could increase its application.

REFERENCES

[1] Mahafzah, K.A.; Obeidat, M.A.; Al-Shetwi, A.Q.; Ustun, T.S. A Novel Synchronized Multiple Output DC-DC Converter Based on Hybrid Flyback-Cuk Topologies. Batteries 2022, 8, pp. 93.

[2] Mahafzah, K.A.; Rababah, H.A. A novel step-up/step-down DC-DC converter based on flyback and SEPIC topologies with improved voltage gain. Int. J. Power Electron. Drive Syst. (IJPEDS) 2023, 14, pp. 898–908.

[3] Chakraborty, S.; Reza, S.M.S.; Hasan, W. Design and analysis of hybrid solar-wind energy system using CUK & SEPIC converters for grid connected inverter application. In Proceedings of the 2015 IEEE 11th International Conference on Power Electronics and Drive Systems, Sydney, NSW, Australia, 9–12 June 2015; pp. 278–283.

[4] D. Ravi, B. Mallikarjuna Reddy, and P. Samuel. (2018). Bidirectional DC To DC Converters: An Overview of Various Topologies, Switching Schemes and Control Techniques.

[5] C. Gupta and M. Das, ‘‘Multiphase interleaved DC–DC converter for fast charging application of electric vehicles,’’ in Proc. IEEE 16th Int. Conf. Compat., Power Electron., Power Eng. (CPE-POWERENG), Jun. 2022, pp. 1–6

[6] A. Benevieri, L. Carbone, S. Cosso, F. Gallione, and S. Hussain, ‘‘Multi-input bidirectional DC–DC converter for energy management in hybrid electrical vehicles applications,’’ in Proc. 13th Int. Symp. Adv. Topics Electr. Eng. (ATEE), Mar. 2023, pp. 1–5

[7] Lin, C.-C; Wu, G.; Yang L.-S. Study of a non-isolated bidirectional DC–DC converter. IET Power Electron.2013, 6, pp. 30–37.

[8] Zhang, Y.; Gao, Y.; Li, J.; Sumner M ;Wang, P.; Zhou, L. High Ratio Bidirectional DC-DC Converter with a Synchronous Rectification H-Bridge for Hybrid Energy Sources Electric Vehicles. J. Power Electron. 2016, 16, pp. 2035–2044.

[9] N. Elsayad, H. Moradisizkoohi, and O. A. Mohammed, “Design and implementation of a new transformerless bidirectional dc-dc converter with wide conversion ratios,” IEEE Trans. Ind. Electron., vol. 66, no. 9, pp. 7067–7077, Sep. 2019.

[10] Savio, D.A.; Juliet, A.V.; Bharatiraja, C.; Padmanaban, S.; Hossain, E.; Blaabjerg, F. Photovoltaic Integrated Hybrid Microgrid Structured Electric Vehicle Charging Station and Its Energy Management Approach. Energies 2019, 12, pp. 168.

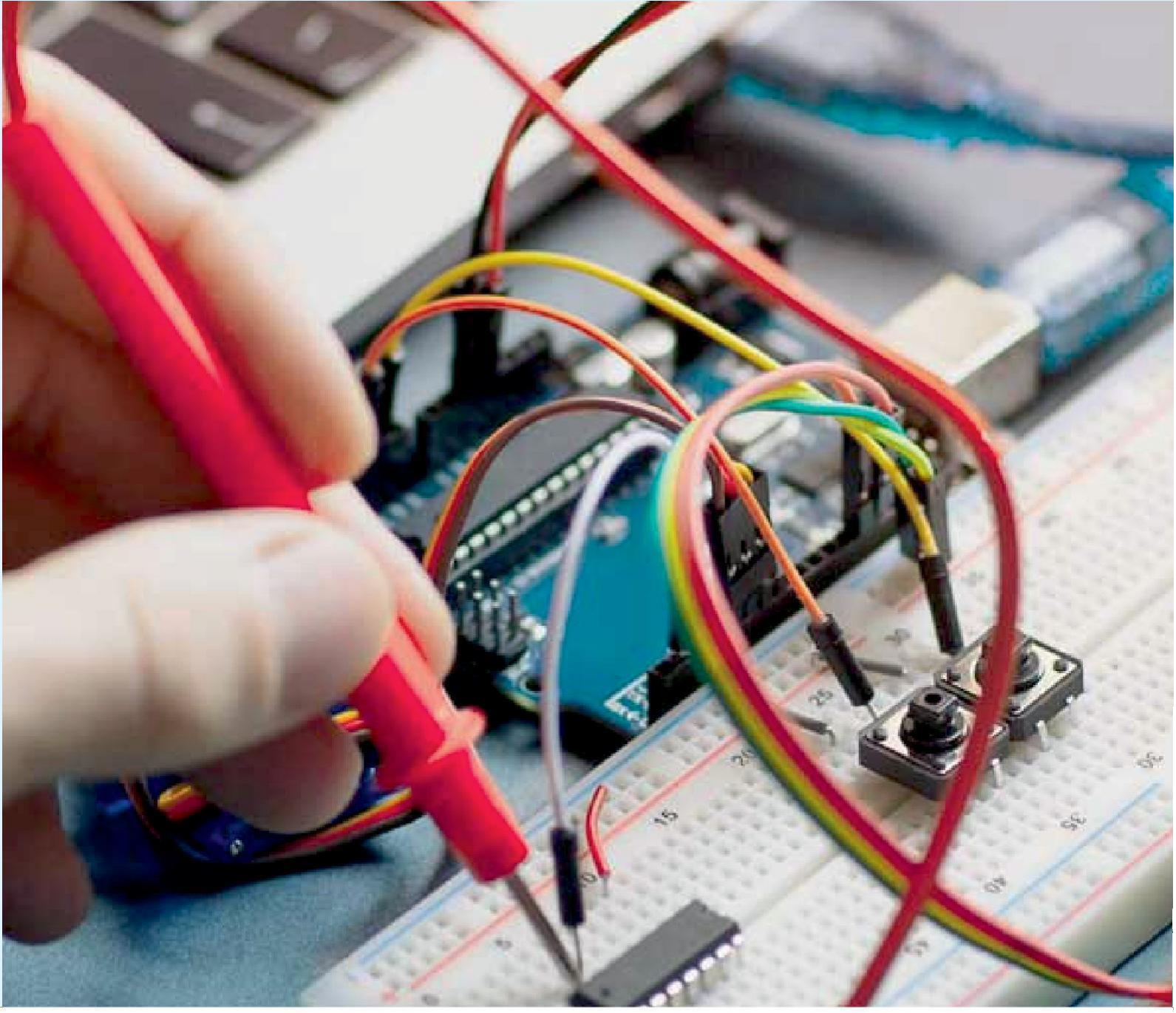

INNO SPACE
SJIF Scientific Journal Impact Factor

doi cross ref

ISSN INTERNATIONAL STANDARD SERIAL NUMBER INDIA

निस्केयर NISCAIR

International Journal of Advanced Research

in Electrical, Electronics and Instrumentation Engineering

9940 572 462 6381 907 438 ijareeie@gmail.com

Scan to save the contact details